Final Technical Report:

Filling a Paleoseismic Data Gap on the San Andreas Fault: Northern Santa Cruz Mountains-San Francisco Peninsula

Principal Investigator:
Gordon Seitz, PhD, CEG
PG 5514, CEG 1718
Engineering Geologist
Seismic Hazard Assessment Program
California Geological Survey
345 Middlefield Road, MS 520
Menlo Park, CA 94025
650.688.6367
Gordon.Seitz@conservation.ca.gov

This research was supported by the U.S. Geological Survey (USGS), Department of the Interior, under USGS Awards G11AP20130. Term of the G11AP20130 Award was 3 March 2011 to 3 March 2017. The views and conclusions contained in this document are those of the Principal Investigators only and should not be interpreted as necessarily representing the official policies, either expressed or implied, of the U.S. Government.

Abstract

A new paleoseismic site on the San Francisco Peninsula was investigated with the objective to fill a data gap along this portion of the San Andreas Fault. Evidence to support the existence of a Peninsula San Andreas Fault segment, with a distinct earthquake history, has been a speculative hypothesis. Other published and non-published paleoseismic records on the peninsula portion of the fault are limited, and appear to have an incomplete recording of earthquakes. The only historical earthquake that has been confidently determined to have ruptured the Peninsular San Andreas Fault section is the 1906 M7.9 San Francisco earthquake. The investigated Monte Bello paleoseismic site is located 76 km and 378 km from the southern and northern ends of that rupture, respectively.

The site is located in the Monte Bello Open Space Preserve, Midpeninsula Regional Open Space District. The San Andreas Fault is expressed as an uphill-facing scarp, about 0.5 m in height across an alluvial fan, and is aligned with three offset channels. Sediments consist of fluvial sands, gravels, marsh deposits, four significant soils layers, and two burn layers, which all provide markers and chronology. Two cross-fault trenches provide evidence for four events during the past 800 years including the 1906 San Francisco earthquake. A preliminary set of seven C-14 AMS dates provide event age estimates that may completely correlate with San Andreas Fault paleoseismic records along the north coast. A permissible alternative allows the penultimate event at the Monte Bello site to be the 1838 earthquake, and pollen and dendrochronological dating is planned to address this possibility.

The interpretation that requires the least amount of assumptions is that the Peninsula section of the San Andreas Fault has exclusively failed in 1906-type earthquakes during the past 800 years, in sync with the North Coast San Andreas Fault section; whereas the Santa Cruz Mountains San Andreas Fault section experiences more frequent moderate size earthquakes in addition to large earthquakes.

Introduction

The purpose of this report is to present the paleoseismic results of an investigation on the San Francisco Peninsula section of the San Andreas Fault. This section of the San Andreas Fault is located nearest to the highest population and infrastructure density in northern California. This investigation was motivated by the fact that this section of the fault significantly lags behind other sections in terms of the existence of robust paleoseismic data, and hence limits our understanding its earthquake behavior. The 1906 M7.9 San Francisco Earthquake was the most recent event that ruptured this fault section. Until this study, one of the only facts we could assert with confidence was that the fault releases strain in great 1906-like quakes. What was not known is whether 1906-like earthquakes are common or the exception.

The initially selected site for this study was the Radonich Ranch in the Santa Cruz Mountains that promised to fill this data gap. Unfortunately, we lost access to the privately owned site.

We found an alternative site that promised to fill the data gap we originally identified in our proposal, and we refer to it as Monte Bello (MB; 37.3077˚N, 122.1545 ˚W) at the Monte Bello Open Space Preserve, Midpeninsula Regional Open Space District, located 32 km north of the Radonich Ranch. The MB site is located in the 75 km long data gap between the Filoli and Grizzly Flat paleoseismic sites (fig.1), a fault section that lacks data in general, compared to the rest of the fault. The active trace of the fault is well-defined by a series of sag ponds and low scarps, cutting a fan deposit. Alluvial fan stratigraphy and abundant dateable material allows excellent chronological resolution of events.

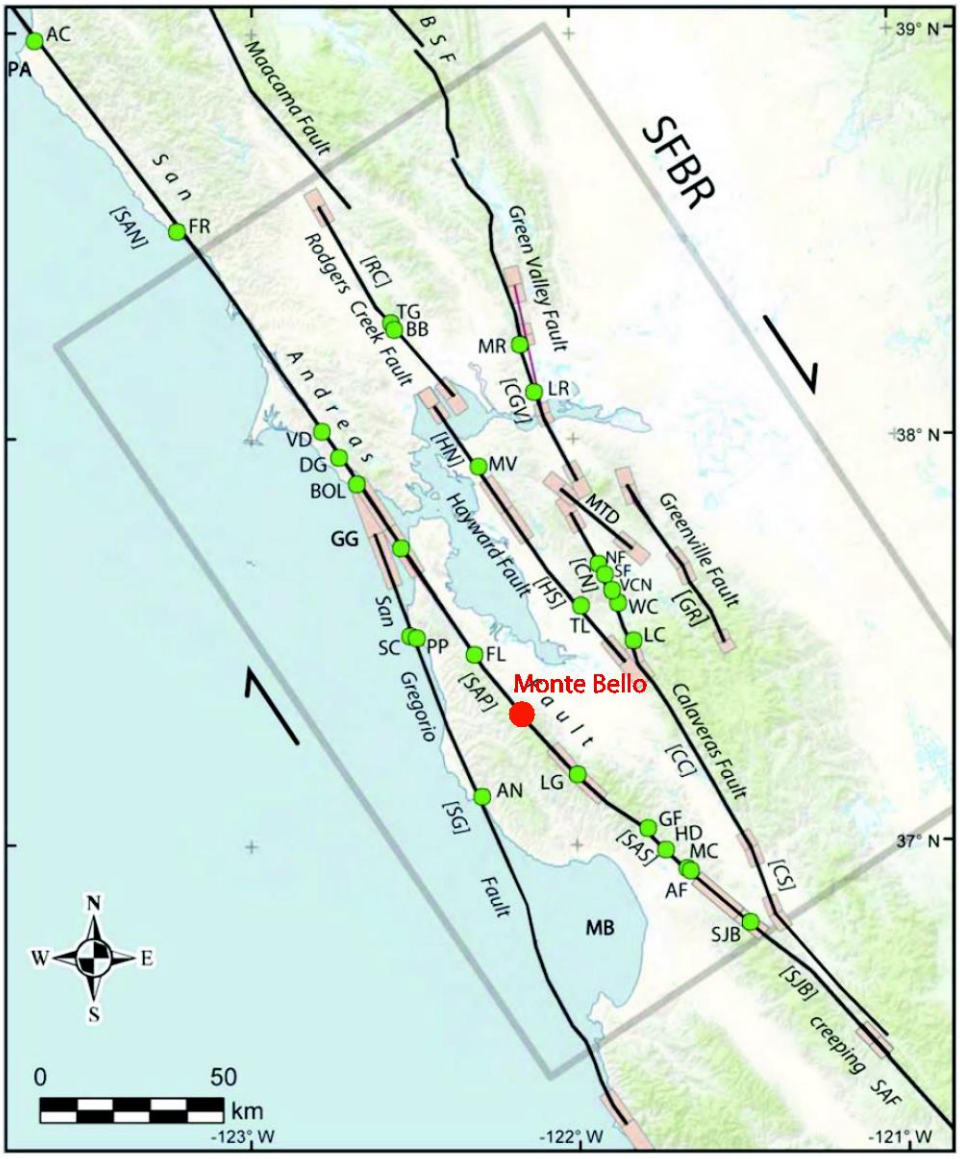

Figure 1. Monte Bello Paleoseismic site location on the San Andreas Fault Peninsular section. Other paleoseismic site locations and other localities referred to in the text are shown with green dots. Tan color rectangles are former fault segment boundaries. Relevant San Andreas Fault paleoseismic sites discussed are in brackets: Monte Bello; VD, Vedanta Marsh; FL, Filoli; GF, Grizzly Flats; HD, Hazel Dell; MC, Mill Canyon; AF, Arano Flat. San Andreas Fault segments indicated and discussed are in brackets: peninsular: SAP; Santa Cruz Mountains: SAS; north coast: SAN. The SFBR rectangle encloses the area defined as the San Francisco Bay Region and has been used by the WGCEP (2003, 2008) to evaluate earthquake probabilities.

Rupture Behavior of the Peninsular Section of the San Andreas Fault

The Peninsular section of the San Andreas Fault fails in large magnitude events but very little is known about the frequency and magnitudes of this earthquake behavior. This sparse paleoseismic data set leads to broad uncertainties in hazard forecasts. Current rupture scenarios are less informed because we simply cannot evaluate the possibility of various modes of fault behavior without longer and better-located records of past earthquakes.

The Working Group on California Earthquake Probabilities (WG03; 2003) defined fault segments along the Peninsular San Andreas Fault section, and then asserted rupture scenarios to calculate rupture probabilities. Although the 1906 earthquake ruptured through the WG02-recognized segment boundary at Los Gatos (Prentice and Schwartz, 1991), 50% of the rupture scenarios prepared by them included rupture terminations at this boundary. The WG02 defined this segment boundary based on a change of trend in the fault, the northern margin of the 1989 Loma Prieta earthquake, and variability in the distribution of geodetically determined slip in the 1906 earthquake (Thatcher and Lisowski, 1987). Even though the 1989 M6.9 Loma Prieta earthquake did not rupture the San Andreas Fault (Prentice and Schwartz, 1991; WG02, 2003), and was attributed to a separate seismic source it did influence Sam Andreas Fault rupture probabilities of the WG02. However, there is no geologic evidence that this defined boundary has ever controlled the extent of a rupture on the San Andreas Fault. in fact, when the 1906 rupture is referred to as being a multi-segment rupture in this area, it may appear less meaningful, because the boundary implied to be a rupture boundary, has been assumed rather than observed.

The northern extent of the Peninsular San Andreas Fault segment is generally considered to be just north of the Golden Gate at the intersection of the San Gregorio and San Andreas Faults. The results of this investigation allow a direct correlation of paleoseismic records on the peninsular and the north coast fault sections in order to evaluate this “segment” boundary.

1838 Earthquake

The 1838 earthquake was the first recognized major (>M7) Bay area earthquake since the founding of the Mission San Francisco Delores (Toppozada et al., 2002). Based largely on the analysis of historical shaking intensities, various workers have placed this quake onto different portions of the San Andreas Fault, and assigned significantly different magnitudes ranging from M6.8 to M7.5. Louderback (1947), and later Sykes and Nishenko (1984) agreed that because shaking intensities were greater at Monterey than San Francisco as compared to 1906, the event must have extended further south than the 1906 rupture extent. Lindh (1983) and the

Working Group California Earthquake Probabilities (WGCEP, 1990) concluded that the quake resulted from a 60 km, M7 rupture centered on the Loma Prieta area. Tuttle and Sykes (1992) further extended the rupture ~ 50 km to the southeast resulting in a M7.2 event. In 1998 Toppazada and Borchardt concluded the entire fault section SAP (San Andreas Fault Peninsular)-SAS (San Andreas Fault Santa Cruz Mountains) was involved, 140 km, equating to a ~M7.5. Bakun (1999) also interpreted shaking reports with a different view on the competence of buildings and concluded that an M6.8 had occurred. While it seems reasonable that the 1838 earthquake occurred on the Peninsula fault section, there are no unequivocal observations placing the 1838 event on the San Andreas Fault.

Schwartz et al. (1998) did not recognize evidence in trench exposures for this earthquake at Grizzly Flat, south of Loma Prieta. On the other hand, Hall et al. (1999) interpreted an offset alluvial deposit as having an excess displacement compared to reported 1906 values (2.5m), and hence assigned a slightly lesser 1.6m of slip to an older event which they interpreted to be the 1838 earthquake.

Selected Paleoseismic Data Relevant to the Peninsula San Andreas Fault Behavior

A brief review of relevant paleoseismic records from north to south follows, sites are shown on figure 1. For a more detailed summary see Schwartz et al. (2014).

Vedanta Marsh

In a highly detailed description of faulting and stratigraphy at the Vedanta Marsh, Zhang et al. (2006) present interpretations for the timing of events, with their preferred model of the penultimate event between 1680 and 1740. Their two events preceding the penultimate events are dated at 1350 to 1440, and 1290 to 1380, respectively.

Fioli

This Fioli paleoseismic site is has provided the only published slip rate determination for the SAP fault section (Hall et al. 1999). The event data contribution is limited to an assertion that an excess displacement compared to reported 1906 values (Lawson, 1908) is due to the 1838 earthquake. Although this is consistent with their chronological data, the error bounds permit the slip to be assigned to a much older prehistoric event, or to be solely due to the 1906 displacement.

Grizzly Flat

At the Grizzly Flats site, Schwartz et al. (1998) interpreted a series of alluvial sands and silts deposited since the mid- 1660s to be offset by only the 1906 rupture. The age of the penultimate event is not directly constrained by subsurface observations

at this site. Schwartz et al. (1998) combined trench and tree-ring observations from a nearby stump and placed the penultimate rupture between 1632 and 1659.

Hazel Dell

Streig et al. (2014) found evidence for four events including the 1906 earthquake at the Hazel Dell site. Historical constraints from pieces of saw cut wood helped refine the event age estimates, and resulted in an age range of 1840 to 1890 for their event 2 and 1815 to 1890 for event 3, with a poorly resolved event 4 several hundred years earlier. They interpreted event 3 to be the 1838 earthquake, and by reinterpreting the Grizzley Flats observations they allow for the possibility of 1838 having ruptured through that site.

Mill Canyon

At the Mill Canyon site (Fumal, 2012), the most recent surface-rupturing event is the 1906 San Francisco earthquake, and it is well expressed as a series of in-filled fissures and small scarps. In addition to the1906 event observations, evidence was found for three events since about 1500. Radiocarbon ages of detrital charcoal suggest an age of the penultimate earthquake of 1711-1770, with a mean date of 1750. Support for this age comes from a 1.5 m deep fissure that formed during this earthquake. It was sampled for Erodium pollen, an imported plant which can provide a timeline. Erodium pollen was not found and would have been present at this site by 1838 in the fill of a fissure formed during an earthquake. Event 3 at Mill Canyon has a mean date of 1690 (Fumal, 2012). Additionally, Fumal (2012) used OxCal to model the radiocarbon dates from Grizzly Flats and presented his own structural interpretation of the trench logs. He suggested that in addition to the 1906 event, there could be two other ruptures, one of which correlates with the penultimate event at Mill Canyon.

Offshore San Andreas Fault Turbidite Record

Based on offshore coring, Goldfinger et al. (2007) identified and correlated 15 turbidites between the Golden Gate and Point Arena, a distance of 280 km. Goldfinger et al. (2007) interpreted the turbidites as earthquake triggered, based on four observations: (1) individual turbidites extend over long distances; (2) 1906 shaking triggered turbidities that can be seen in the cores; (3) the average interval between the past 15 turbidities is approximately 200 years, which is in reasonable agreement with the average land interval of 248 years for the past 11 ruptures at Vedanta (Zhang et al., 2006); and (4) the calculated age of each of the five most recent is generally coincident with paleoearthquakes dated on land. Along-strike correlation suggests that at least 8 of the most recent 10 events ruptured at least the entire North Coast segment to near San Francisco. Based on radiocarbon dating of foraminifera and analysis of sedimentation rates, (Goldfinger et al., 2007, 2008) calculate the penultimate turbidite formed between 1647 and 1819, with a

preferred date of 1724. Although many issues concerning the validity of this record remain, it has many very compelling aspects. If true, it supports the notion that the San Andreas Fault releases its strain in great earthquakes and not in a Gutenberg-Richter-like distributions of events with no characteristic magnitude. Furthermore, this may provide the longest record of San Andreas Fault events. It is clear that to fully adopt this record of events as a proxy for the San Andreas Fault, longer onshore, onfault paleoseismic records are needed for validation. Although the San Gregorio fault, may "contaminate" the offshore San Andreas Fault shaking record south of the Golden Gate, a total budget of strong shaking remains.

Slip Rate

For the 150 km long SAP-SAS fault section, only one longer-term geologic slip rate determination at the Fioli site (figure 1) of 17 ± 4 mm/yr during the past 2070 ± 120 years exists (Hall et al, 1999). At Arano Flat (fig.1) Fumal et al. (2003) determined a short-term (<600 yr) slip rate of 22.5 ± 2 mm/yr. South of SAS, along the creeping section of the San Andreas Fault, Perkins et al. (1989) determined a slip rate of 22 ± 5 mm/yr over the past 800 years. Geodetic models support a high slip rate in the 16.8-21 mm/yr range (d'Alesio et al., 2005; Geist and Andrews, 2000; respectively). The uncertainties of these models, combined with the lack of geologic data motivated the WG02/08 use of a constant rate of 17 ± 4 mm/yr.

For 160 km fault section between the Vedanta site (Zhang et al., 2006) near the southern end of the North Coast section to the Mill Canyon and Arano Flat sites (Fumal et al., 2003) near the southern end of the SAS section, there is only one longer-term geologic slip rate determination of 17 ± 4 mm/yr (Hall et al, 1999). Ongoing research by Blisnuik (pers. com.) within 10 km of the Monte Bello site suggests a higher slip rate of ~20 mm/year, based on cosmogenic surface exposure dating of offset landforms. These higher slip rate estimates may be significant, because they suggest that the difference in slip rates between the north coast and the peninsular sections may be less than previously thought. Recurrence data from sites bounding this 75 km data gap are limited and summarized later in this report.

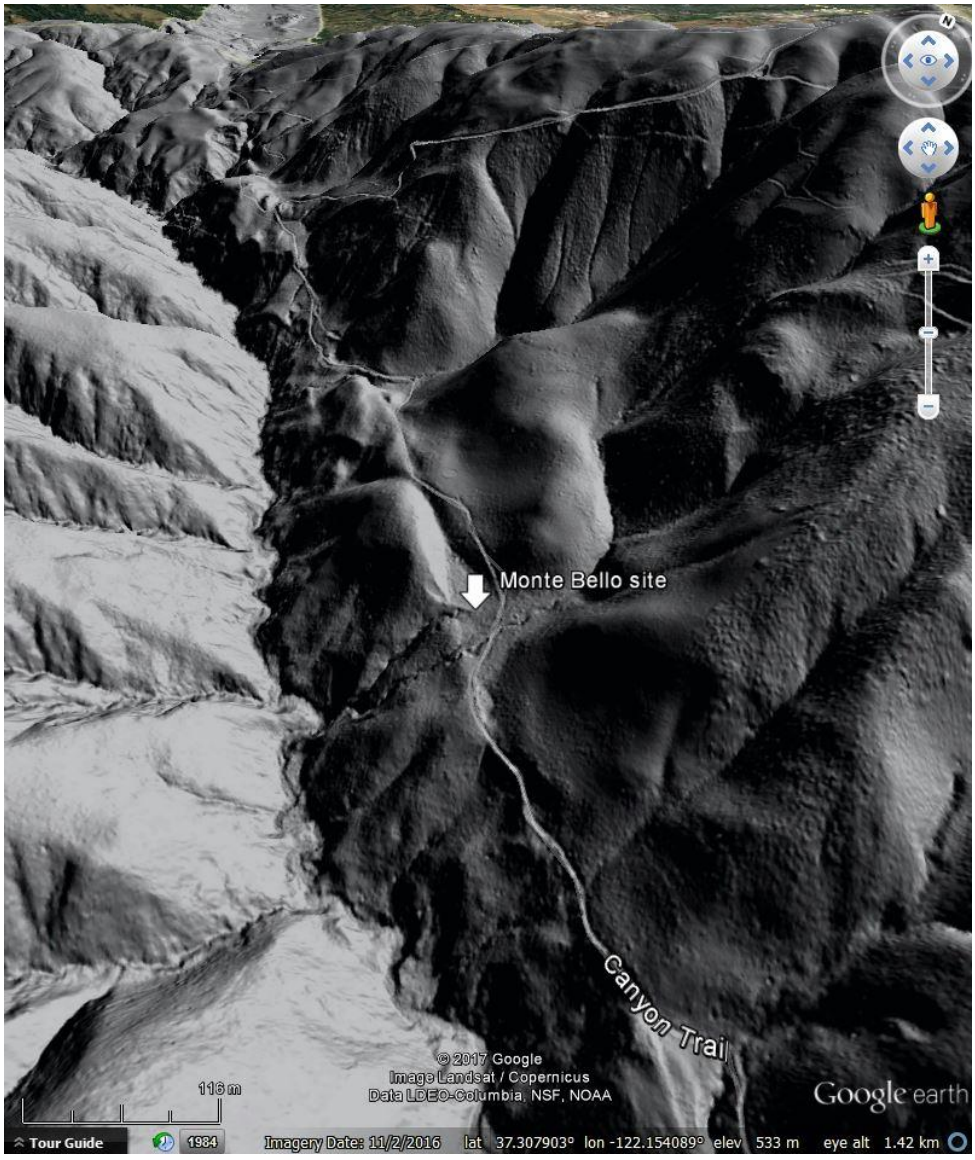

Figure 2. Oblique Lidar Hillshade Image of the San Andreas Fault with the Monte Bello Site Location. (MB; 37.3077˚N, 122.1545 ˚W)

Monte Bello Paleoseismic Site

Setting

The Monte Bello Paleoseismic site is located in the Monte Bello Open Space Preserve, part of the Midpeninsula Regional Open Space District (fig.1, 2). We selected the site using Earthscope lidar (http://www.opentopography.org) data acquired along the northern San Andreas Fault. In the Monte Bello Preserve, the active trace of the San Andreas Fault is well expressed with typical strike-slip geomorphology, including sag ponds, shutter ridges and offset drainages. The site is located along the slope on the east side of a large-scale fault-controlled linear valley. In the vicinity of the site the fault has formed a side-hill bench that varies in width ranging up to approximately 100 meters. The down slope margin of this flatter bench is generally delineated by the San Andreas Fault scarp or shutter ridges. At the trench site (fig.3), the fault is well expressed by an uphill, east-facing scarp 0.5 m in height that has formed across an active alluvial fan. This fan is being deposited by Bay Creek, and is bounded by two sag ponds, north and south of the trench site. East of the fault Bay Creek is incised about 1.5 meters, and is right-laterally offset about 7 m. Two additional offset channels exist 17 m and 67 m further north. We selected to trench a fairly open area north of the 17 m channel (fig. 3). This trench area is bounded on the north by a wet overgrown meadow and the forested area includes large oak and bay trees. Further north (fig.3) a sag pond has formed against a shutter ridge, with the southern outlet of the pond being artificially dammed.

Methods

The Earthscope lidar combined with field reconnaissance led to the identification of the Monte Bello site. Because the site is largely under a dense canopy of trees, the bare earth lidar has relatively low resolution. Additionally, the site was covered with dead wood. To document the fine-scale geomorphology prior to excavation we manually cleared the site of wood and grasses, and used a ladder to photograph the site with several hundred nearly vertical images taken with a Nikon D300 SLR. These images were processed with a “Structure from Motion” (SfM) software package (Agisoft Photoscan Professional v.1.25). Placed targets provided scale and orientation and we surveyed perimeter targets to correct for topographic edge effects. Three versions of the SfM product are presented here: 1) a perspective mosaic model (fig. 4), 2) a perspective hillshade version (fig. 5), and 3) a digital elevation model (fig. 6; DEM). The trench locations were imaged in the same fashion and added to the original pre-excavation DEM. The objective of this SfM survey was to capture microgeomorphology related to the most recent earthquakes, that is often too fragile to survive the trenching operation. Trench logging confirmed the scarp locations identified with the geomorphology.

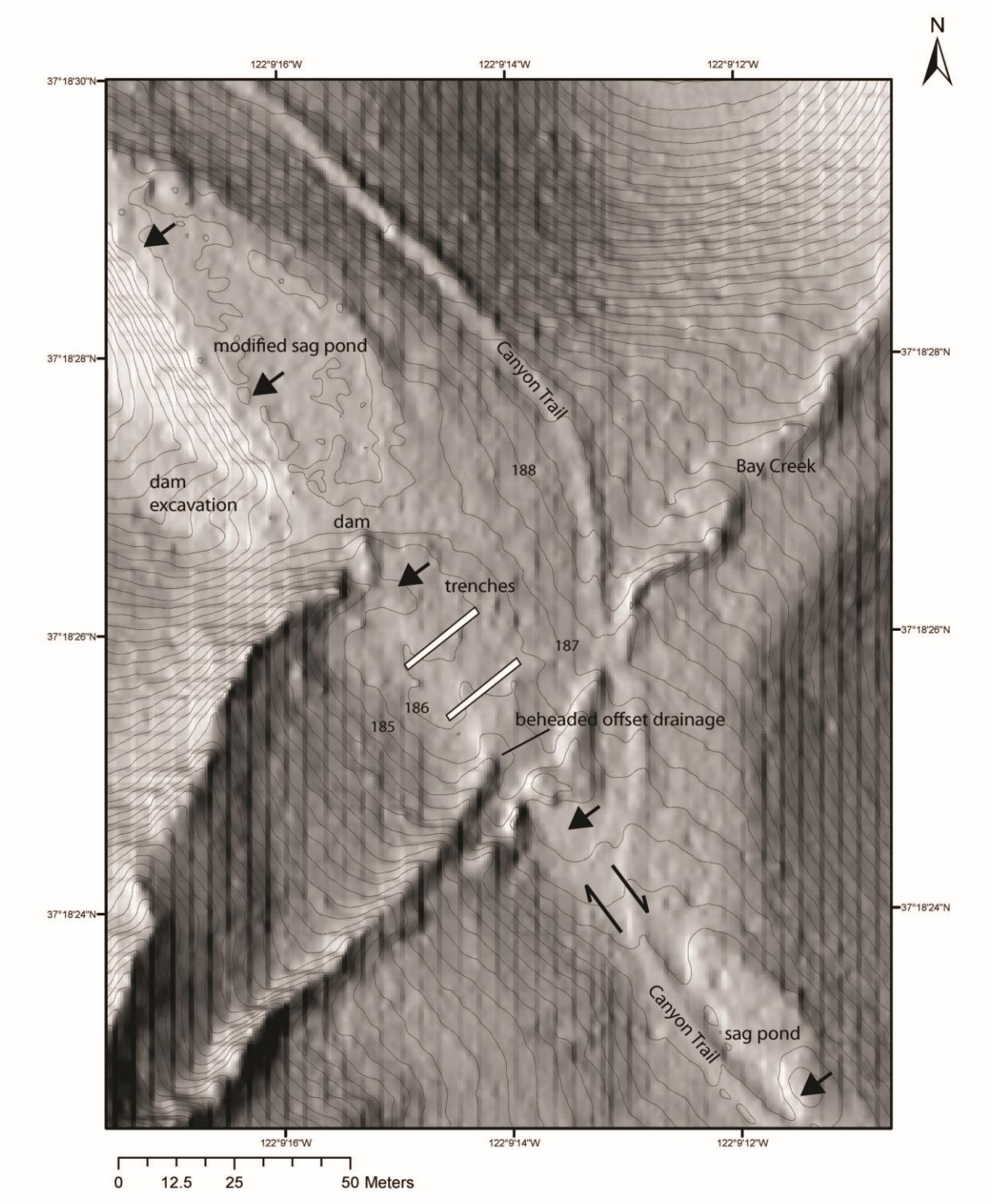

Figure 3. Hillshade Site Map from Lidar DEM. This map shows the trench location schematically; exact locations are shown on fig. 6. Arrows indicate location of the fault. Channel offsets are addressed in the text. (MB; 37.3077°N, 122.1545 °W)

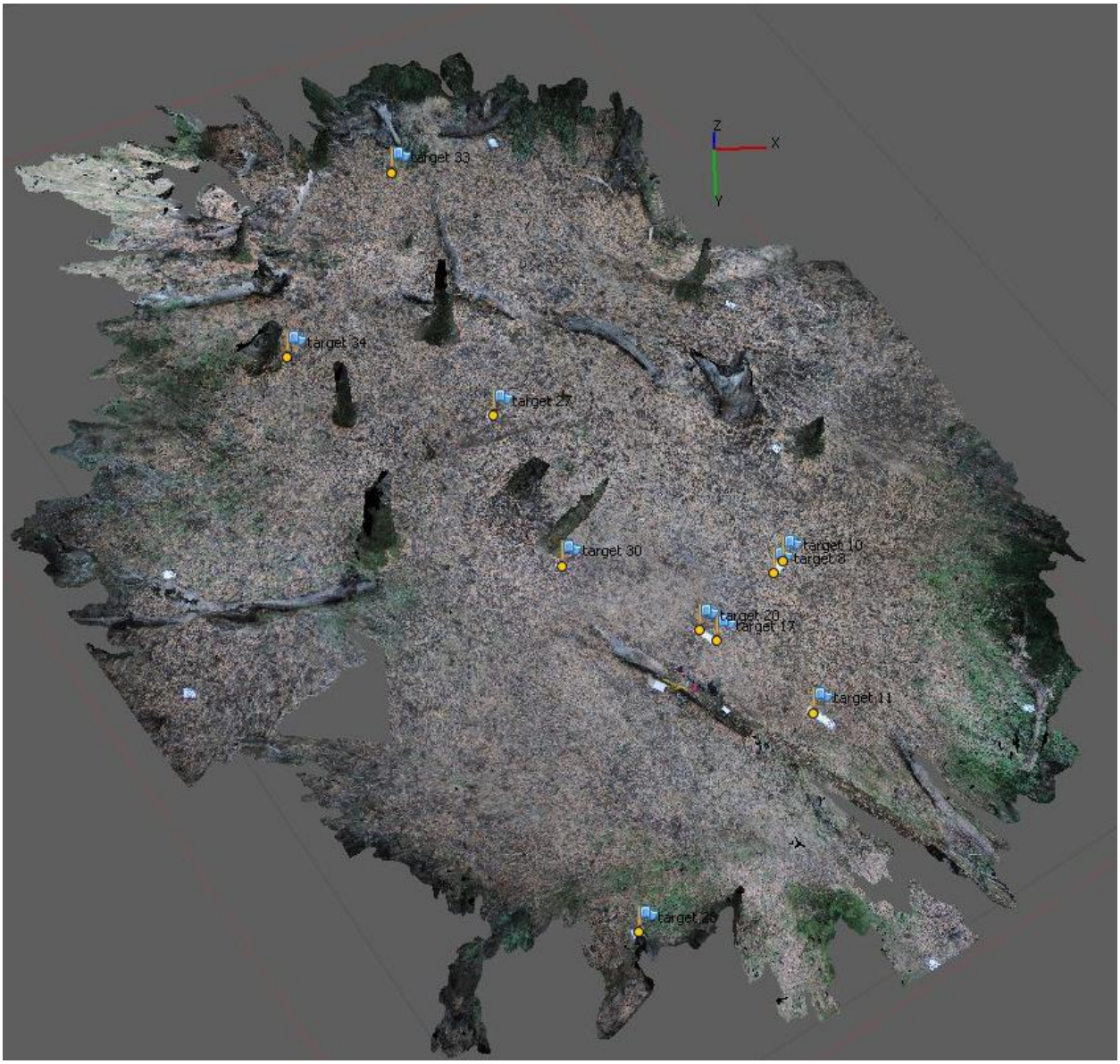

Figure 4. Agisoft Photoscan SfM Perspective Site model. This image is a working step to produce a high resolution pre-excavation DEM. Ground control targets are indicated as yellow dots with blue flags.

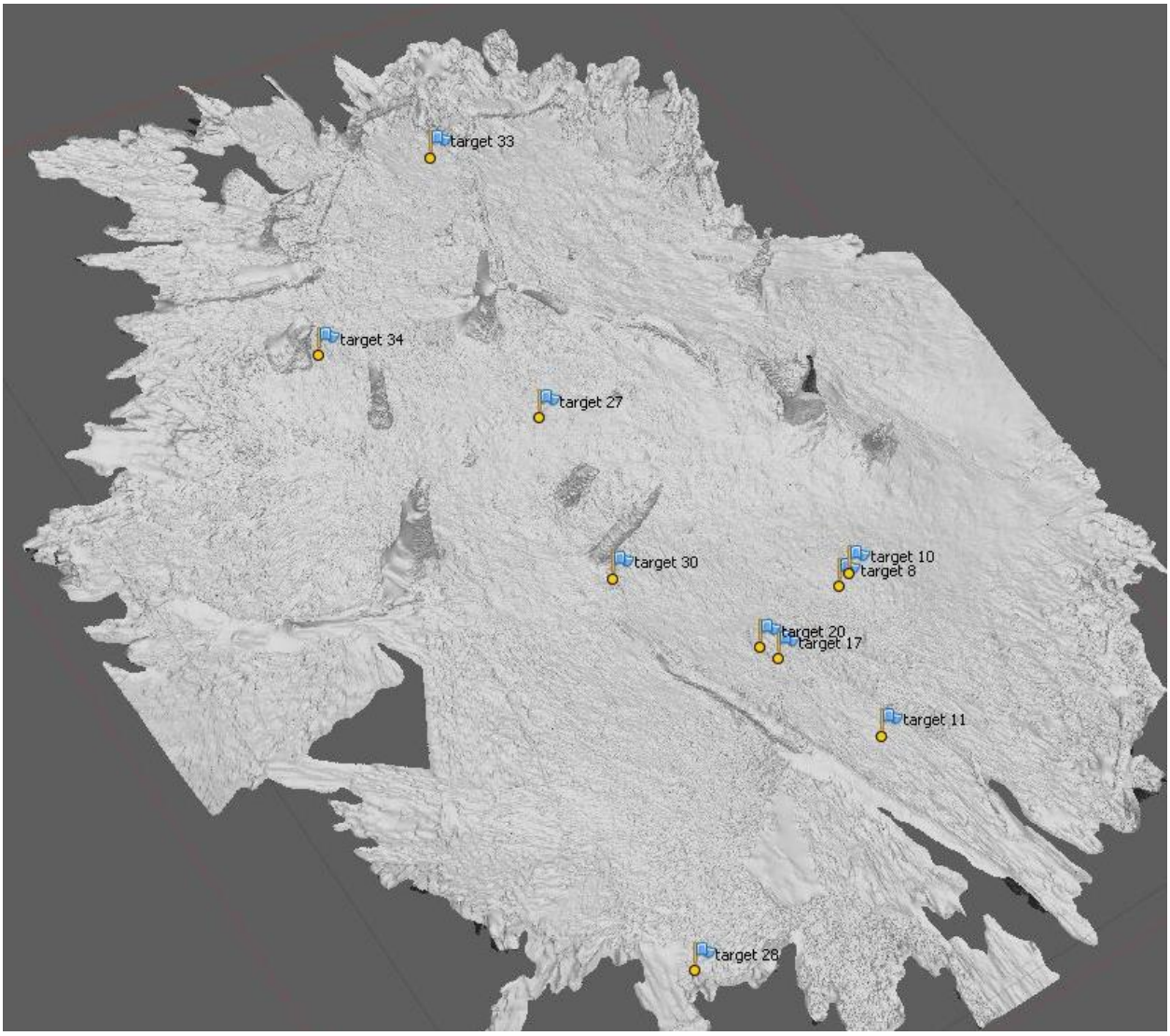

Figure 5. Agisoft Photoscan SfM Perspective Site model Hillshade. This is a working step to produce a high resolution pre-excavation DEM. Ground control targets are indicated as yellow dots with blue flags.

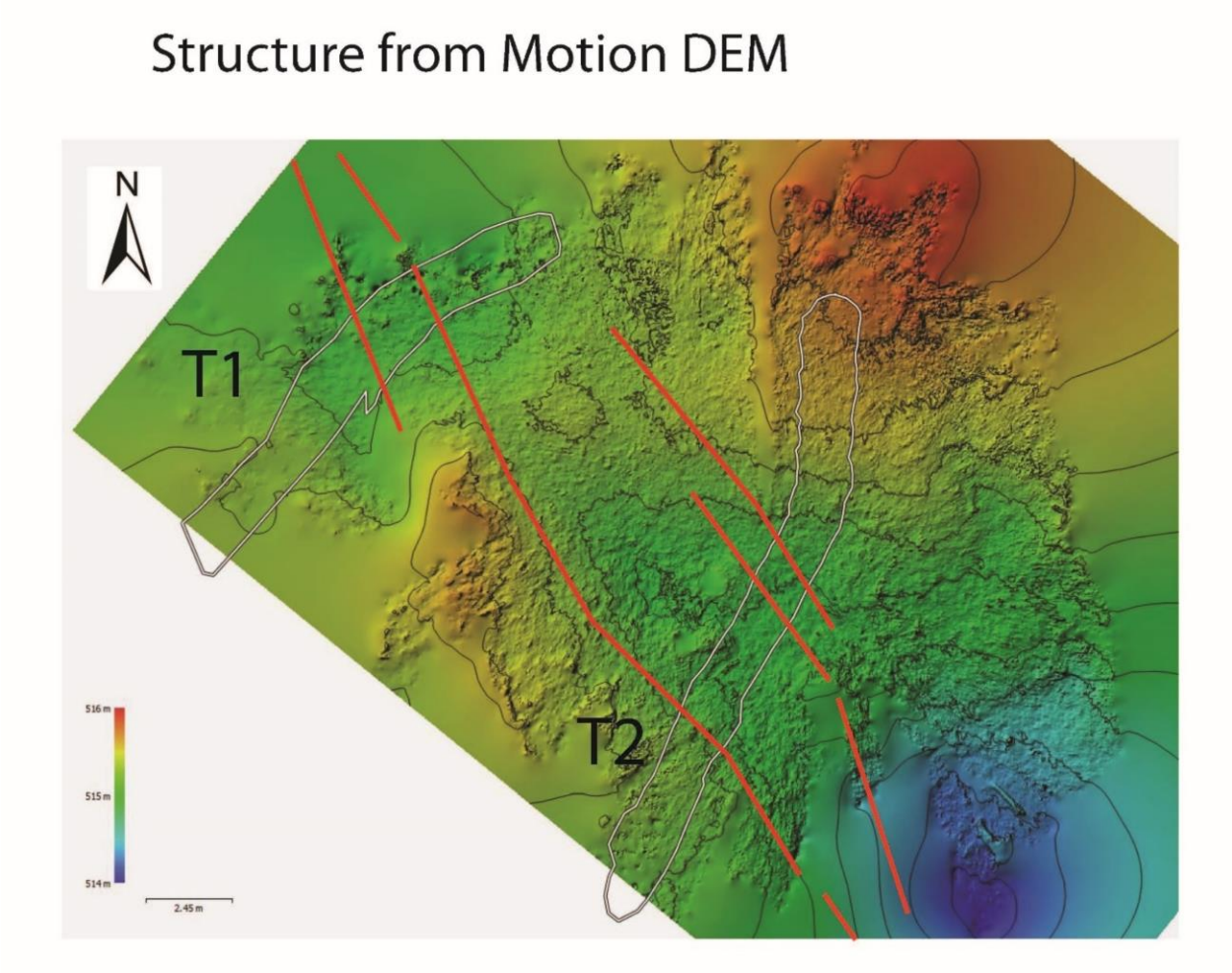

Figure 6. Agisoft Photoscan DEM. The faults displayed in red were interpolated from the trench exposures and geomorphology. The elevations are indicated by colors and contours; trench locations are shown by gray polygons. These are exact trench locations for the site illustrated in fig.3.

Two fault perpendicular trenches were excavated as shown on the DEM in fig. 6. The northern trench, T1, encountered shallow water at 1-meter depth, and concerns for collapse resulted in a shorter trench towards the east. Both trenches required constant dewatering, by siphon and by pumps. The trench walls were cleaned by washing with water, scarping, brushing and leaf blower. Contacts were marked with colored nails, and C-14 samples were collected and marked with blue ribbons. Multiple sets of images were taken at different times in order to find the optimal lighting conditions. Because of the dense canopy, a hand-held studio LED light panel provided the most uniform and highest resolution image results of the trench walls.

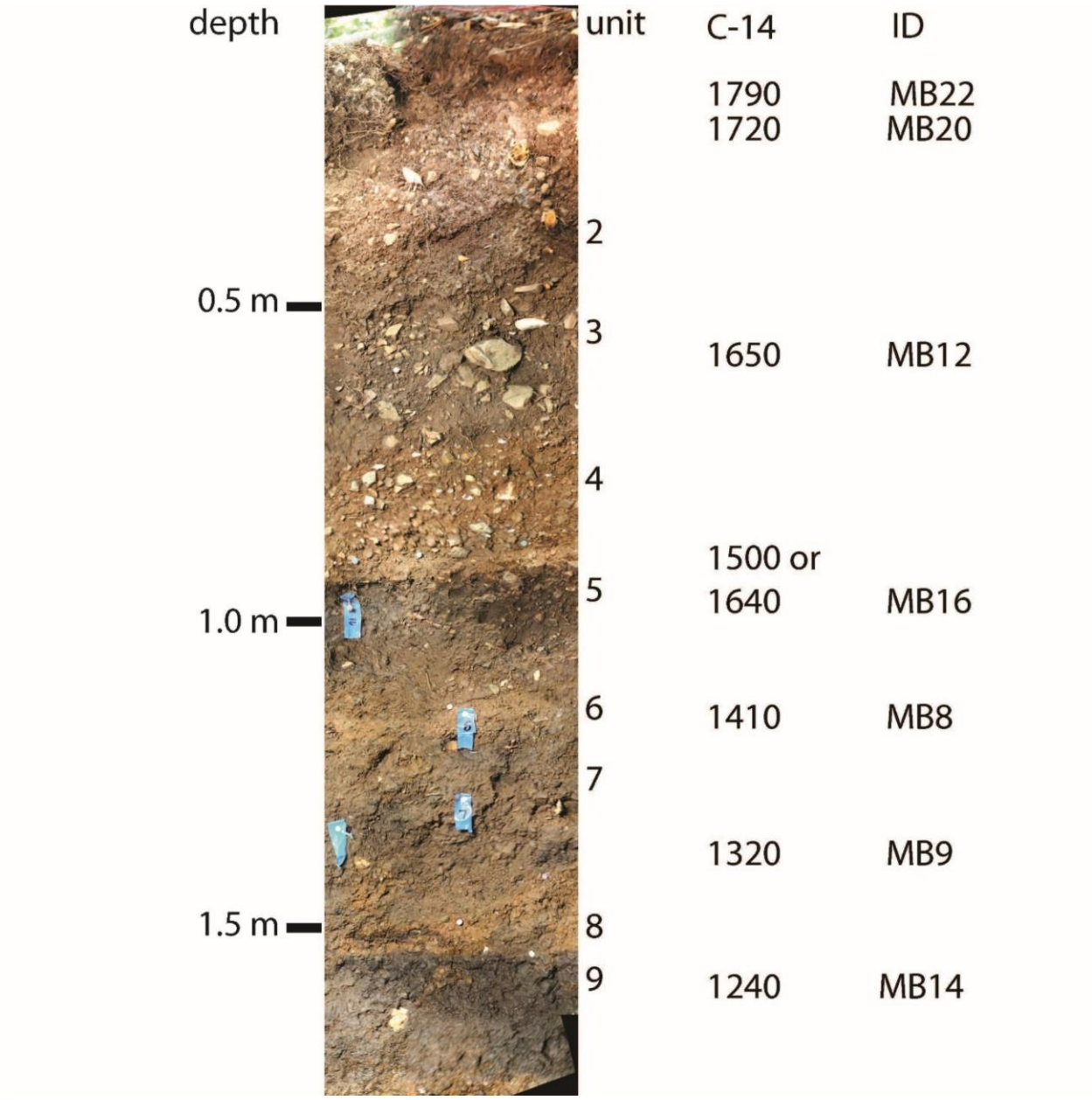

Figure 7. Reference Stratigraphic Column. Alluvial fan sediments record multiple events at the site and consist of: 2-sandy silt, 3-soil, organic-rich silty sand with gravel, 4-channel gravel, 5-organic-rich soil, silty sand, 6-burn, tan sandy silt, 7-soil, organic-rich sandy silt, 8-burn, tan silty gravel, 9-soil, organic-rich silty sand. C-14 ages are the calibrated mode in years A.D., laboratory results are provided in Table. 1.

Stratigraphy

The trenches exposed alluvial fan sediments consisting of sands, gravels and marsh deposits faulted against older, Pleistocene (?) gravels, and highly weathered Franciscan bedrock. The event stratigraphy is shown in fig. 7. The odd numbered units 3, 5, 7, and 9 are organic-rich soils indicating relative landscape stability. The cause for this stability could be the landscape position relative to the active channel of Bay Creek just south of the excavations (fig.3) or a relatively dry period. These soil units provide clear markers throughout the site, and they consist of silty sand with variable amounts of sub-angular gravels. The older soils (5, 7, and9) have higher organic contents. Datable materials are abundant throughout the section and include detrital charcoal, and scattered animal bone fragments. Preservation of these datable materials is better than average due to the high groundwater level. Unit 6 is a fine sandy silt that is a burn (soil burned by fire), it is laterally discontinuous and often occurs as fragmented pods at the boundary between soils 5 and 6. Unit 8 consists of an orange tan sandy gravel, which in places also has burn characteristics.

Fault Structure and Event Stratigraphy

The fault is expressed consistently in both the trenches and the geomorphology as a high lateral displacement fault at the base of a low, uphill-facing continuous scarp, and an along-fault trough bounded by a secondary fault zone exists 6 m to the northeast, and trends nearly parallel to the main fault. This secondary fault zone is only fully exposed in T2. The geomorphic channel offsets indicate that most of the lateral displacement occurs along the main fault, however some units, such as the unit 4 gravel, are not exposed on the west side of the secondary fault zone in T2, suggesting lateral displacements of greater than 1.5 m, the trench width, have taken place. The faulting pattern, as shown on fig. 6, is a rough en echelon left-stepping fault trace, which in places is recognized in the surface geomorphology.

Geomorphic Channel Offsets

The geomorphic channel offsets at the site (fig. 3) are 7 m, 17 m and 67 m. The 7 m offset includes a smaller 3-4 m depression that appears to represent the most recent event, which would result in 4 m of lateral slip remaining for the penultimate event. Seven meters appears too large for the 1906 earthquake given Lawson's (1908) observation of about 1-2 m 2.5 miles north of the site at Page Mill Road. The 17 m offset results in an additional 10 m for the pre event 2 offset, again this appears large for an individual event, so one can speculate that the 10 m may have resulted from two or more events. These channels are only incised about 1.5 m on the alluvial fan that we trenched just 20 m to the north, so a reasonable assumption is that these channels have formed during the approximate same time span as the exposed stratigraphy. If this speculation is correct, it results in offsets of 3 m for 1906, 4 m for event 2, and a combined 10 m for events 3 and 4. This scenario is

consistent with the slip rate estimates for the fault of about 20mm/year, which should average about 4 m of slip each 200 years. These offsets are all comparable in amount to the 1906 displacements in this area

SW NW

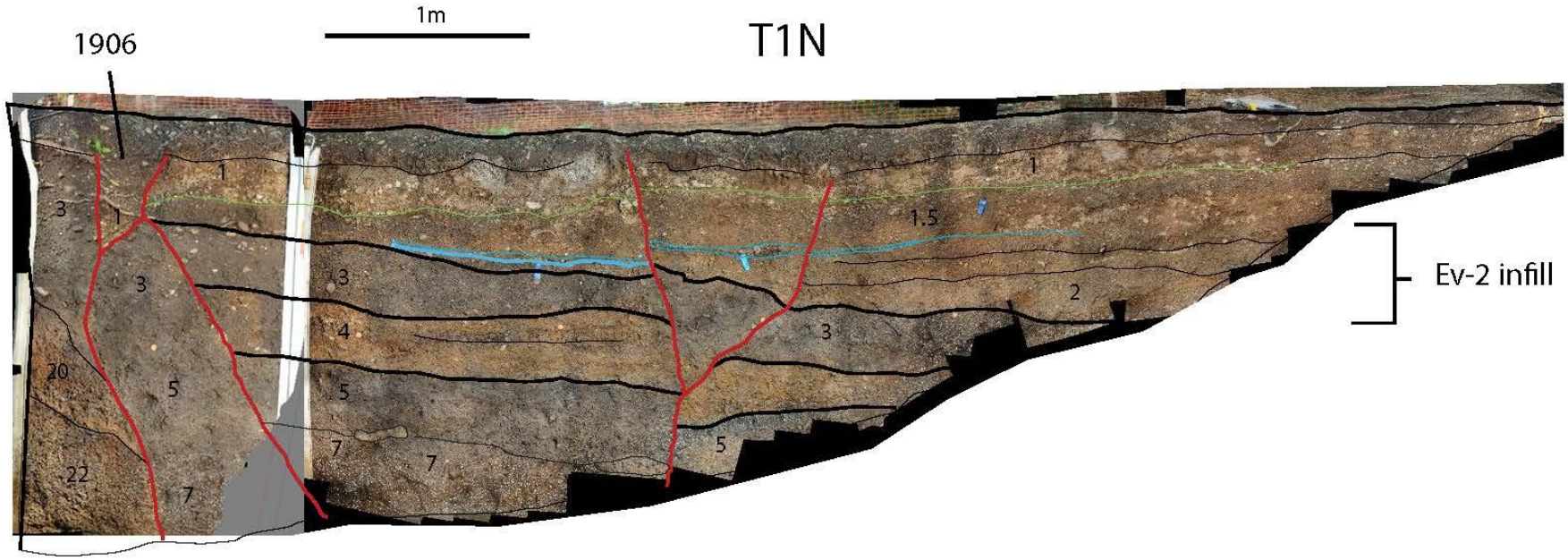

Figure 8. Trench 1 North Wall Log. Base is a Agisoft Photoscan image mosaic. All fault breaks that extend higher than unit 3 are attributed to the 1906 earthquake. This exposure shows clear evidence for 1906 and event 2. Older events have not been resolved.

SW NE

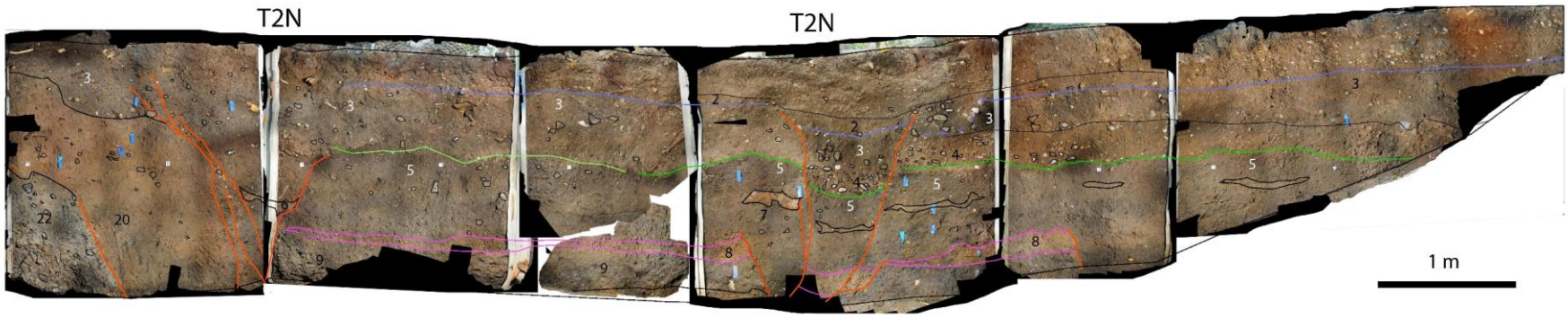

Figure 9. Trench 2 North Wall Log. Base is a Agisoft Photoscan image mosaic. Sedimentary units are shown with black or white numbers. The event horizons are colored coded: event2- blue, event 3-green, event 4-magenta.

NE SW

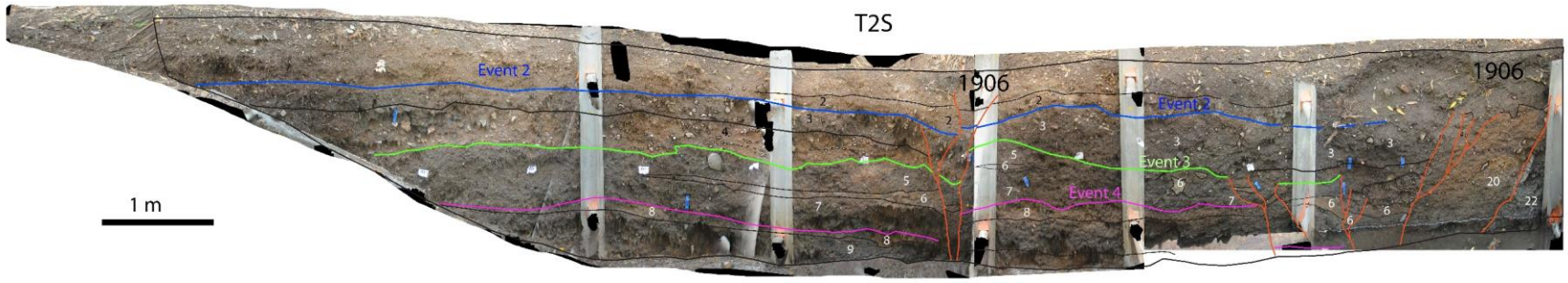

Figure 10. Trench 2 South Wall Log. Base is a Agisoft Photoscan image mosaic. Sedimentary units are shown with black or white numbers. The event horizons are colored coded: event2- blue, event 3-green, event 4-magenta.

1906

The most recent event the 1906 earthquake is well documented along this portion of the fault. Lawson (1908) describes clear surface rupture with 1.5 m to 3 m of displacement on Page Mill Road 2.5 miles north of the site. In the trench exposures there are clear faults extending up to the base of the surface soil. In Trench 1, at the main fault, the westernmost fault shown in the trench logs (figs. 8), the highest stratigraphic level breaks terminate in a tan gravelly unit, that is the source of fissure fill material of the most recent rupture. In Trench 2 (figs., 9,10), the 1906 event is indicated by faults in the secondary zone breaking unit 2.

Event 2

Both trenches provide evidence for the penultimate event with an event horizon at the top of soil unit 3. In T1 unit 3 is faulted by the secondary fault 3 m east of the main fault, and down warped to the east. Units 2 and younger were deposited onlapping across the deformed unit 3. The units above unit 3 were subsequently faulted by the 1906 event on the main fault and the secondary trace. The 1906 secondary faulting shows an apparent down to the east sense of displacement, indicated by a blue marked horizon on fig. 8. In T2 the penultimate event is expressed on both trench walls as a thickening of the overlying unit 2 across the eastern secondary fault zone.

Event 3

The event horizon is the top of unit 5. In T2 north wall (fig.9) in the main fault zone there is a fissure that terminates at the top of unit 5. In T2 south wall (fig.10) upward terminating faults and a distinct down warp of unit 5 is observed. The overlying unit 3 is deposited in this low onlapping unit 5 to the east and buttressing against the main fault to the west.

Event 4

This event has the least evidence due to our limited exposure at this stratigraphic level with an event horizon at the top of unit 8. In T2 south in the main fault zone (fig. 10), there are west dipping faults that show a distinct down-section increase of separation. In T2 north (fig.9) in the eastern secondary fault zone there are upward terminating faults with overlying continuous layers.

Chronology

The sediments exposed in the trenches include abundant datable materials, such as detrital charcoal, in place burned charcoal layers, fire pits, shells, and animal bone fragments. We mainly used relatively large charcoal pieces with a particle long axis greater than 5 mm. P.I. Seitz visited LLNL/CAMS and

conducted the C-14 AMS laboratory pretreatment for the samples presented in Table 1. A suite of seven samples were dated. However, we collected over sixty samples and additional dating is being considered to reduce the event age uncertainties. A long detrital charcoal residence time or reworking does not appear to be an issue because the sample ages are all in the correct stratigraphic order. However, a systematic age offset cannot be ruled out at this time. The event ages (fig. 11) were modeled using the Oxcal program (Bronk Ramsey, 1994), which provides an efficient web-based tool that allows a controlled method to incorporate multiple types of chronological data. The constraints that we used in the Oxcal model are the most recent event is assumed to be 1906, and the stratigraphic order of all samples, event ages were calculated between modeled sample ages. We sampled the younger stratigraphic section for pollen analysis, which may help determine if event 2 could be the historical 1838 earthquake.

Sample Name	CAMS#	Location	Unit Number	Material	^{14}C Age	±	d^{13}C
MB-8	175639	T2S	6	Charcoal	565	30	-25.1
MB-9	175646	T2S	7	Charcoal	515	25	-25.1
MB-12	175640	T2S	3	Charcoal	265	25	-25.5
MB-14	175641	T2N	9	Charcoal	800	25	-24.2
MB-16	175642	T2N	4	Charcoal	245	30	-23.7
MB-20	175645	T1	2	Charcoal	165	25	-25.3
MB-22	175643	T1	1.5	Charcoal	220	25	-23.5

Table 1. Radiocarbon data from Monte Bello Open Space Preserve Trenches 1 and 2.

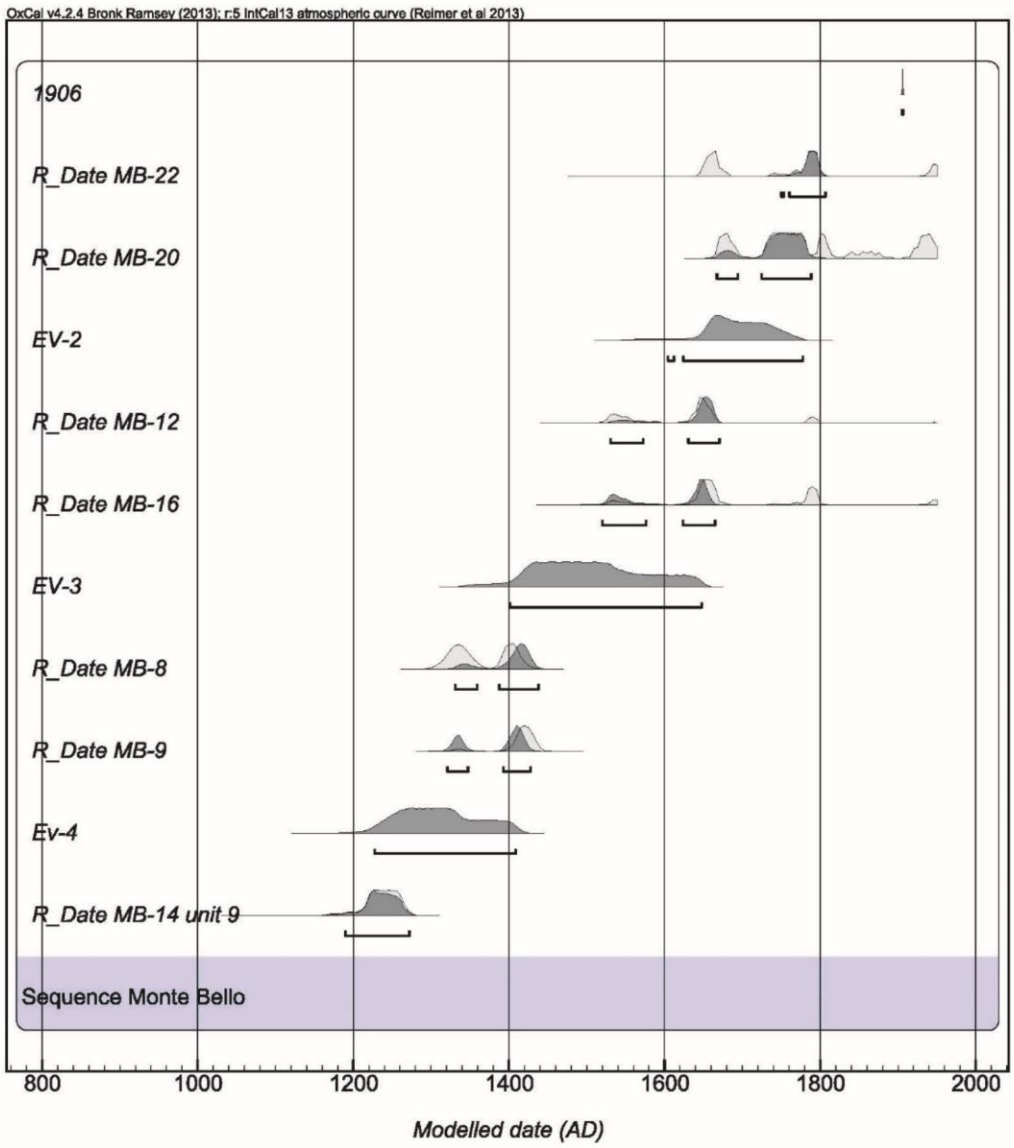

Figure 11. Chronological Age Model with Event Age Estimates.

Discussion

The preliminary chronology at the Monte Bello site has significant individual event age uncertainties, however, the number of four events for the overall time span of 800 years is robust. Paleoseismic records in the Santa Cruz Mountains clearly show more frequent earthquakes, likely due to moderate size earthquakes nucleating near the seismically active creeping portion of the fault. Examples of these moderate size earthquakes include the historical 1838 and 1890 earthquakes. The event chronology at the Monte Bello site indicates the penultimate event occurred at 1700 AD, and although one cannot completely rule out the historical1838 earthquake, it appears unlikely. Another observation that supports the notion that each of the Monte Bello site events are large 1906-like events are the large offsets of geomorphic channels discussed previously. It is permissible that the event record correlates completely with the North Coast San Andreas Fault paleoseismic records (Zhang et al., 2006), including the offshore turbidite record (Goldfinger et al., 2007), suggesting these represent long 1906-like ruptures. At this point we cannot prove that each of the past four Monte Bello events correlates directly with each of the past four North Coast San Andreas Fault events, however we certainly cannot say they do not correlate.

It appears that the interpretation that requires the least amount of assumptions is that the Peninsula section of the San Andreas Fault has exclusively failed in 1906-type earthquakes during the past 800 years, in sync with the North Coast San Andreas Fault; whereas the Santa Cruz Mountains San Andreas Fault section experiences more frequent moderate size earthquakes in addition to large 1906-like earthquakes.

REFERENCES

d'Alesso, M.A., Johanson, I.A., Bürgmann, R., Schmidt, D.A., Murray, M.H., 2005, Slicing up the San Francisco Bay Area: Block kinematics and fault slip rates from GPS-derived surface velocities, J. Geophys. Res., v. 110, no. B06403, p1-19.

Bakun, W.H., 1999, Seismic activity of the San Francisco Bay region, Bull. Seim. Soc. Am. 89, 764-784.

Bronk Ramsey, C. 1994. Analysis of Chronological Information and Radiocarbon Calibration: The Program OxCal. *Archaelogical Computing Newsletter,* 41, 11-16.

Fumal, T. E. , 2012. Timing of large earthquakes during the past 500 yearsalong the Santa Cruz mountains segment of the San Andreas Fault at Mill Canyon, near Watsonville, California, Bull. Seismol. Soc. Am. 102, 1099–1119.

Fumal, T.E. Heingartner, G.F. Samrad, L., Dawson, T.E., Hamilton, J.C., and Baldwin, J.N., 2003, Photomosaics and Logs of Trenches on the San Andreas Fault at Arano Flat near Watsonville, California: U.S. Geological Survey Open-File Report 03-450, Version 1.0

Geist, E.L., and Andrews, D.J., 2000, Slip rates on San Francisco Bay area faults from anelastic deformation of the continental lithosphere, J. Geophys. Res., v. 105, no.B11, p. 25,543-25,552.

Goldfinger, C., Morey, A.E., Nelson, C.H., Guterrez-Pastor, J., Johnson, J.E., Karabanov, E., Chaytor, J., Eriksson, A., Shipboard Scientifc Party, 2007, Rupture lengths and temporal history of significant earthquakes on the offshore and north coast segments of the Northern San Andreas Fault based on turbidite stratigraphy, Earth and Planetary Science Letters, 254, p.9-27.

Hall, N.T., Wright, R.H., and Clahan, K.B., 1999, Paleoseismic studies of the San Francisco peninsula segment of the San Andreas Fault zone near Woodside, California: Journal of Geophysical Research, v. 104, no. B10, p. 23,215-23,236.

Lindh, A.G., 1983, Preliminary assessment of long-term probabilities for large earthquakes along selected segments of the San Andreas system in California, U.S. Geol. Surv. Open-File Rept. 83-63, 1-15.

Lawson, A. C. ,1908, The California Earthquake of April 18, 1906, Reportof the State Earthquake Investigation Commission, Vol. 1, Carnegie Inst., Washington, 451 pp.

Louderback, G.D., 1947, Central California earthquakes of the 1830's, Bull. Seism. Am., v.37,p 33-74.

Perkins, J.A., Sims, J.D., and Sturgess, S.S., 1989, Late Holocene Movement along the San Andreas Fault at Melendy Ranch: Implications for the distribution of fault slip in California: Journal of Geophysical Research, v. 94, p. 10,217-10230.

Prentice, C.S., and D.P. Schwartz, 1991, Re-evaluation of 1906 surface faulting, geomorphic expression, and seismic hazard along the San Andreas Fault in the southern Santa Cruz mountains, Bull. Seis. Soc. Amer., v. 81, 1424-1479.

Schwartz, D.P., Lienkaemper, J.J, Hecker, S.,Kelson, K. I.,Fumal, T.E., Baldwin, J.N., Seitz, G.G., Niemi, T.M., The Earthquake Cycle in the San Francisco Bay Region: A.D. 1600-2012,

2014, Bulletin Seis. Soc. Amer., vol. 104, no. 3, p. 1299-1328.

Schwartz, D.P., Pantosti, D., Okumura, K., Powers, T., and Hamilton, J., 1998, Paleoseismic investigations in the Santa Cruz Mountains: Implications for the recurrence of large magnitude earthquakes on the San Andreas Fault: Journal of Geophysical Research, v. 103, p. 17,985-18,001.

Seitz, G., Biasi, G., and Weldon, R. 1997, The Pitman Canyon paleoseismic record suggests a re-evaluation of San Andreas Fault segmentation, Journal of Geodynamics, ed. Michetti, A.M.,and P.L. Hancock, v. 24, n.1-4, p. 129-138.

Streig, A. R., T. E. Dawson, and R. J. Weldon II , Paleoseismic evidence of the 1890 and 1838 earthquakes on the Santa Cruz Mountains section of the San Andreas Fault, near Corralitos, CA, Bull. Seis-mol. Soc. Am. 104, 285–300, doi: 10.1785/0120130009

Sykes, L.R., and S.P., Nishenko, 1984, Probabilities of occurrence of large plate rupturing earthquakes for the San Andreas, San Jacinto, and Imperial faults, California, J. Geophys. Res. 89, 5905-5927.
Thatcher, W.,and Lisowski, M., 1987, Long-term seismic potential of the San Andreas Fault southeast of San Francisco, J. Geophys. Res., 92,4771-4784.

Toppozada, T.R., and Borchardt, G., 1998, Re-evaluation of the 1836 "Hayward Fault" earthquake and the 1838 San Andreas Fault earthquake: Seismological Society of America Bulletin, v. 88, p. 140-159.

Toppazada, T.R., Brauum, D.M., Reichle, M.S., Hallstrom, C.L. 2002, San Andreas Fault Zone, California:≥5.5 Earthquake History, Bull. Seis. Soc. Amer., v. 92, no.7, p. 2555-2601.

Tuttle, M.P., and L.R. Sykes, 1992, Re-evaluation of several large historic earthquakes in the vicinity of the Loma Prieta and peninsular segments of the San Andreas Fault, California, Bul. Seis. Soc. Amer., v. 82, 1802-1820.

Wesnousky, S.G., 2008, Displacement and Geometrical Characteristics of Earthquake Surface Ruptures:Issues and Implications for Seismic_Hazard Analysis and the Process of Earthquke Rupture: Seismological Society of America Bulletin, v. 98, no. 4, p. 1609-1632.

Working Group on California Earthquake Probabilities, 1990, Probabilities of large earthquakes in the San Francisco Bay Region, California: U.S. Geological Survey Circular, p. 51.

Working Group on California Earthquake Probabilities, 2003, Earthquake Probabilities in the San Francisco Bay Region: 2002–2031: U.S. Geological Survey Open-File Report 03-214.

Working Group on California Earthquake Probabilities, 2008, The Uniform California Earthquake Rupture Forecast, Version 2 (UCERF 2): U.S. Geological Survey Open-File Report 2007-1437, 95 p.

Zhang, H., Niemi, T., and Fumal T., 2006, A 3000-year record of earthquakes on the northern San Andreas Fault at the Vedanta marsh site, Olema, California: Seismological Research Letters, v. 77, p. 176.